

Supporting Information

Biocompatible and Light-Penetrating Hydrogels for Water Decontamination

Gloria Guidetti,^a Demetra Giuri,^a Nicola Zanna,^a Matteo Calvaresi,^a Marco
Montalti,^{a*} and Claudia Tomasini^{a*}

^a Dipartimento di Chimica Giacomo Ciamician – Università di Bologna
Via Selmi 2 – 40126 Bologna – Italy

Contents

Preparation of hydrogels 1 (H), 2 (H-T), 1 (H), 2 (H-T), 4 (HR), 5 (HR-T), 6 (HR-TG)	Pages S2-S3
Characterization of hydrogels 1 (H), 2 (H-T), 1 (H), 2 (H-T), 4 (HR), 5 (HR-T), 6 (HR-TG)	Pages S4-S5
Figure S1. Strain dependence for hydrogels 1-3 .	Page S6
Figure S2. Frequency dependence for hydrogels 1-3 .	Page S7
Figure S3. Emission spectra (540-700nm) of the 1 (H), 2 (H-T), 4 (HR), 5 (HR-T), 6 (HR-TG) by excitation at $\lambda_{exc} = 530$ nm	Page S8
Figure S4. Excitation spectra in the range 330-600nm at $\lambda_{em} = 620$ nm of the 1 (H), 2 (H-T), 4 (HR), 5 (HR-T) and 6 (HR-TG) .	Page S8
Figure S5. Comparison of the RhB emission lifetime decays in the ns timescale for 4 (HR), 5 (HR-T) and 6 (HR-TG) . The system is excited at $\lambda_{exc}=408$ nm with a detection at $\lambda_{em}=530$ nm.	Page S8
Figure S6. Fluorescence anisotropy measurements for the samples 4 (HR), 5 (HR-T) and 6 (HR-TG)	Page S9
Pseudo first order analysis of the photodegradation kinetics	Page S10
Figure S7. log plots of $c(t)/c_0$ versus t as measured for 4 (HR), 5 (HR-T) and 6 (HR-TG) .	Page S10
Figure S8. Hypothesis of the mechanism of RhB degradation pathway.	Page S11

Preparation of hydrogels 1 (H), 2 (H-T), 1 (H), 2 (H-T), 4 (HR), 5 (HR-T), 6 (HR-TG)

Materials - All chemicals and solvents were purchased from Sigma-Aldrich, VWR or Iris Biotech and were used as received. Acetonitrile was distilled under inert atmosphere before use. MilliQ water (Millipore, resistivity = 18.2 mΩ.cm) was used throughout.

Synthesis of TiO₂-NPs – TiO₂ nanoparticles were synthesized in water solution by means of Pluronic® F127 (Plur) non-ionic surfactants following an industrial patented protocol ¹. Titanium tetraisopropoxide (TTIP, purity ≥97.0%), has been chosen as a TiO₂ precursor. Pluronic® F127 (10% w/w) and concentrated HCl (1,4mL) were placed in a 500 mL round bottom flask with 250 mL of Millipore ultrapure water (resistivity 18.2 MΩ·cm at 25°C). The solution was heated up at 50 °C and was stirred for almost 30 minutes. Then 1,5% w/w of TTIP was added very rapidly. A white precipitate was noticed. After 24h stirring at 50° a semi-transparent colloidal solution of TiO₂-NPs (15 mg/ml) was collected.

Synthesis of TiO₂-NPs/graphene – A 15-mL aqueous dispersion was prepared with 9.4 mL of Plur-TiO₂ 15 mg/mL with 15 mg of natural graphite flakes was sonicated in the bath sonicator for 6 hours, stirring for almost 1 minute every 30 minutes. Then, the dispersion was divided in two aliquots of 7,5 mL and it was centrifuged for 5 minutes at 9500 RPM. Then, the 65% of the supernatant was collected for the analysis. A 0.1% Graphene doping was expected to be obtained following the procedure reported in Ref. ².

Synthesis of Fmoc-L-Tyr-D-Oxd-OH – The compound was synthesized from D-Thr and Fmoc-L-Tyr(t-Bu)-OH following a multistep procedure in solution, reported in ref. ³.

Conditions for Gel Formation - A portion of Fmoc-L-Tyr-D-Oxd-OH (5 mg) was placed in a test tube (diameter: 8 mm), then MilliQ water (0.97 mL) and a 1M aqueous NaOH (1.3 equiv.) were added and the mixture was stirred until sample dissolution. For the preparation of the hydrogels, we used the pH change method. This method relies upon the enhanced solubility of Fmoc-Tyr-Oxd-OH at basic pH, followed by a slow decrease of pH by addition of glucono-δ-lactone. The gels were prepared as shown in the following Scheme (SS1).

Hydrogel	Gelator	1M NaOH (1.3 eq.)	glucono- δ - lactone (1.4 eq.)	RhB (5×10^{-4} M)	TiO ₂ -NPs (0.2 mg/mL)	TiO ₂ -Gr (0.2 mg/mL – 0.1%)
1 (H)	5 mg	12 μ L	2.4 mg	-	-	-
2 (H-T)	5 mg	12 μ L		-	13.5 μ L	-
3 (H-TG)	5 mg	12 μ L		-	-	13.5 μ L
4 (HR)	5 mg	12 μ L	2.4 mg	2 μ L	-	-
5 (HR-T)	5 mg	12 μ L	2.4 mg	2 μ L	13.5 μ L	-
6 (HR-TG)	5 mg	12 μ L	2.4 mg	2 μ L	-	13.5 μ L

Since the solutions containing TiO₂ have a pH \approx 1, we adopt the following procedure, to avoid the formation of non-homogeneous hydrogels:

- the gelator (5 mg) was placed in a test tube, then milliQ water (1 mL) and aqueous 1 M NaOH (12 μ L) were added and the mixture stirred and sonicated in turn for about 10 minutes, until sample dissolution;
- 2 μ L of RhB (5×10^{-4} M) were added to the solution under stirring (only for samples **4**, **5** and **6**);
- 2.4 mg of glucono- δ -lactone were added to all the samples under stirring;
- when the solution reached pH \approx 6, we added the solution containing TiO₂ (only for samples **2** and **5**) and TiO₂-graphene (only for samples **3** and **6**) under stirring, followed by a rapid transfer into cuvette (500 μ L, for photodegradation tests), vials (500 μ L, for preparation of SEM analysis sample) or plate (700 μ L, for rheology analysis).

References

- (1) Baldi, G.; Bitossi, M.; Barzanti, A. Method for the Preparation of Aqueous Dispersions of TiO₂ in the Form of Nanoparticles, and Dispersions Obtainable with This Method. Google Patents April 2013.
- (2) Guardia, L.; Fernández-Merino, M. J.; Paredes, J. I.; Solís-Fernández, P.; Villar-Rodil, S.; Martínez-Alonso, A.; Tascón, J. M. D. High-Throughput Production of Pristine Graphene in an Aqueous Dispersion Assisted by Non-Ionic Surfactants. *Carbon N. Y.* **2011**, *49* (5), 1653–1662.
- (3) Zanna, N.; Merlettini, A.; Tatulli, G.; Milli, L.; Focarete, M. L.; Tomasini, C. Hydrogelation Induced by Fmoc-Protected Peptidomimetics. *Langmuir* **2015**, *31* (44), 12240–12250.

Characterization of hydrogels **1 (H)**, **2 (H-T)**, **1 (H)**, **2 (H-T)**, **4 (HR)**, **5 (HR-T)**, **6 (HR-TG)**

Aerogels Preparation - Some samples of hydrogels **1-3** were freeze dried using a BENCHTOP Freeze Dry System LABCONCO 7740030 with the following procedure: the hydrogel was prepared into an Eppendorf test tube at room temperature. After 16 hours, the samples were deepened in liquid nitrogen for 10 minutes, then freeze-dried for 24 hours *in vacuo* (0.2 mBar) at -50 °C.

Morphological Analysis - Scanning electron micrographs of the samples were recorded using a Zeiss EP EVO 50 field emission gun scanning electron microscope.

Conditions: EHT=20 KeV - Variable Pressure (VP): 100 Pa - Images in secondary electrons (SE)

UV- Vis absorption spectra - UV-Vis absorption spectra (range 200-800nm) are collected by using an optical path of 0.5cm cuvette at 25 with a Cary300 UV-Vis double beam spectrophotometer, having an empty cuvette as a reference.

Rheology - Rheology experiments were carried out on an Anton Paar Rheometer MCR 102 using a parallel plate configuration (25 mm diameter). Experiments were performed at constant temperature of 23 °C controlled by the integrated Peltier system and a Julabo AWC100 cooling system. To keep the sample hydrated a solvent trap was used (H-PTD200). Amplitude and frequency sweep analysis were performed with fixed gap value of 0.5 mm on hydrogel samples prepared directly on the upper plate of the rheometer once the gelation reaction was completed. The samples were prepared the day before the analysis and leaved overnight at controlled temperature of 20 °C to complete the gelation process. Oscillatory amplitude sweep experiments (γ : 0.01–100%) were carried out to determine the linear viscoelastic (LVE) range at fixed frequency of 1 rad·s⁻¹. Once established the LVE of each hydrogel, frequency sweep tests were performed (ω : 0.1-100 rad·s⁻¹) at constant strain within the LVE region of each sample. Thixotropic experiments were conducted on hydrogels **1 (H)**, **2 (H-T)** and **3 (H-TG)** by applying consecutive deformation and recovery steps. The deformation step was performed by applying to the gels a constant strain above the LVE region of each sample for a period of 7 minutes. The recovery step was performed by keeping the sample at constant strain within the LVE region for 7 minutes. The cycles were performed multiple times at fixed frequency of 1 rad/s.

Emission, excitation and fluorescence anisotropy - Spectra were collected with an Edinburgh FLS920 fluorimeter equipped with a photomultiplier Hamamatsu R928P, and the samples were analyzed in disposable cuvettes with optical path length of 0.5 cm. Emission: $\lambda_{exc} = 530$ nm; λ_{em} : 540-700nm. Excitation: $\lambda_{exc} = 330-600$ nm, $\lambda_{em} = 620$ nm. Fluorescence anisotropy: $\lambda_{exc} = 530$ nm; λ_{em} : 550-650nm

Emission lifetime - Spectra were collected with an Edinburgh FLS920 fluorimeter equipped with a photomultiplier Hamamatsu R928P. Excitation was performed with the aid of a diode pulsed laser with $\lambda_{exc} = 408$ nm with $\lambda_{em} = 570$ nm, on a 0-50 ns emission time range.

Photodegradation tests - The kinetic analysis was carried on monitoring the degradation of Rhodamine B (RhB) in a sequence of fluorescence spectra with Horiba Fluoromax-4 spectrofluorimeter with the parameters reported in the following Scheme (SS2):

λ_{exc} (nm)	340
Excitation slit (nm)	20
λ_{em} (nm)	450-700
Emission slit (nm)	1
Cycles	100 (no delay)
Scan speed (nm/s)	0.1
Stirring speed (RPM)	1000
Lamp	Xenon Lamp
Optical path	0.5cm

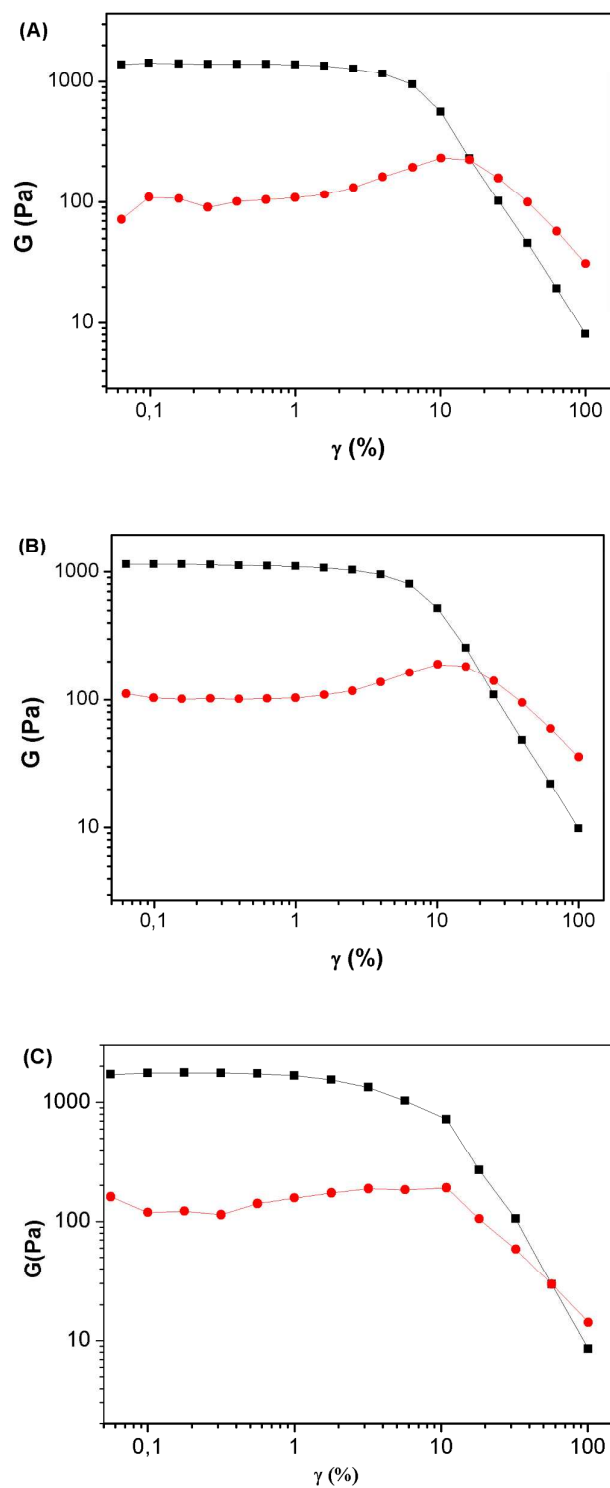


Figure S1. (A) Strain dependence of storage modulus (square) and loss modulus (circles) for hydrogel 1. (B) Strain dependence storage modulus (square) and loss modulus (circles) for hydrogel 2. (C) Strain dependence storage modulus (square) and loss modulus (circles) for hydrogel 2. The analyses were performed on the gel about 20 hours after the gelation began.

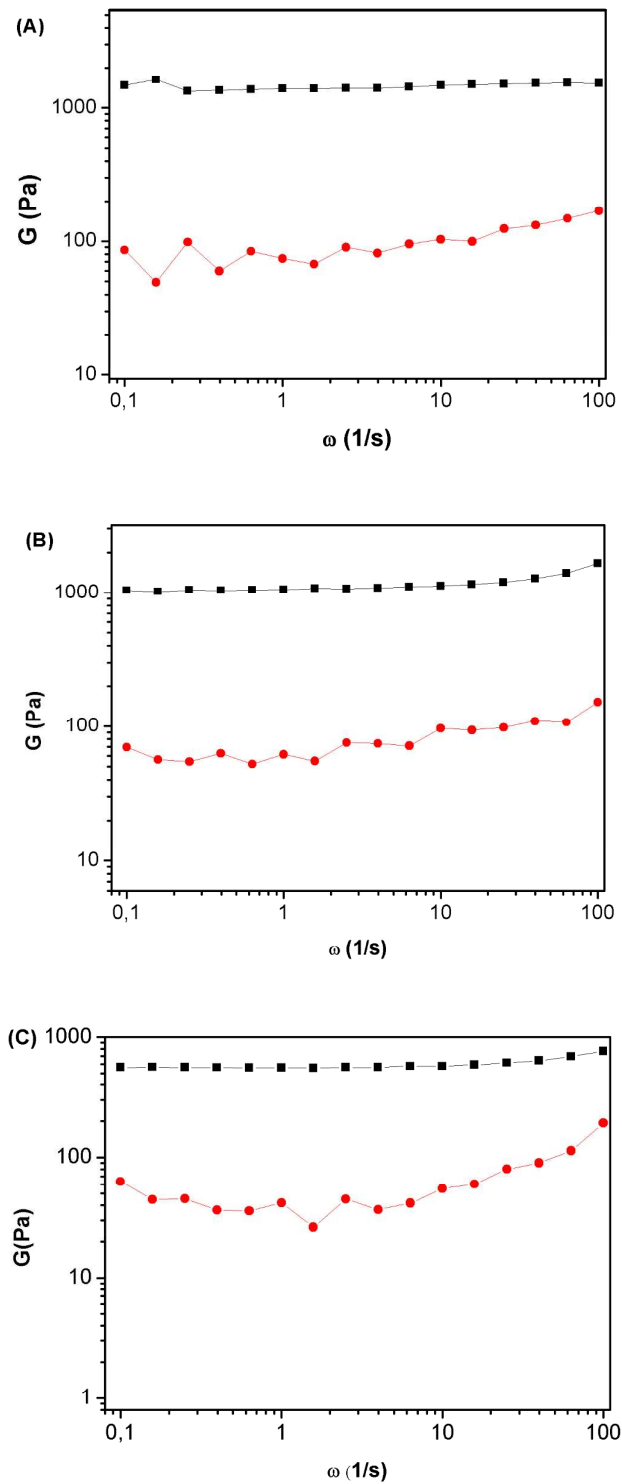


Figure S2. (A) Frequency dependence of storage modulus (square) and loss modulus (circles) for hydrogel **1**. (B) Frequency dependence of storage modulus (square) and loss modulus (circles) for hydrogel **2**. (C) Frequency dependence of storage modulus (square) and loss modulus (circles) for hydrogel **3**. The analyses were performed on the gel about 20 hours after the gelation began.

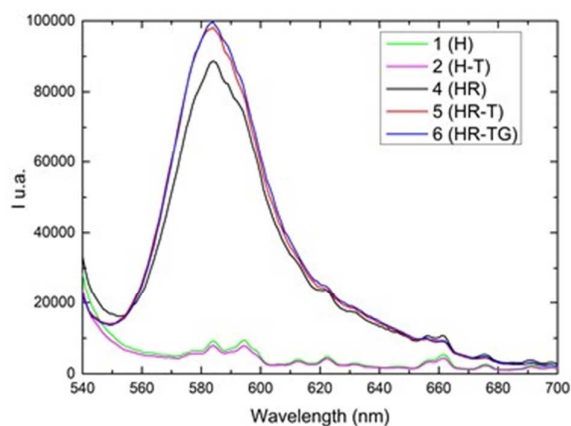


Figure S3. Emission spectra (540-700nm) of the **1 (H)**, **2 (H-T)**, **4 (HR)**, **5 (HR-T)**, **6 (HR-TG)** by excitation at $\lambda_{exc} = 530$ nm.

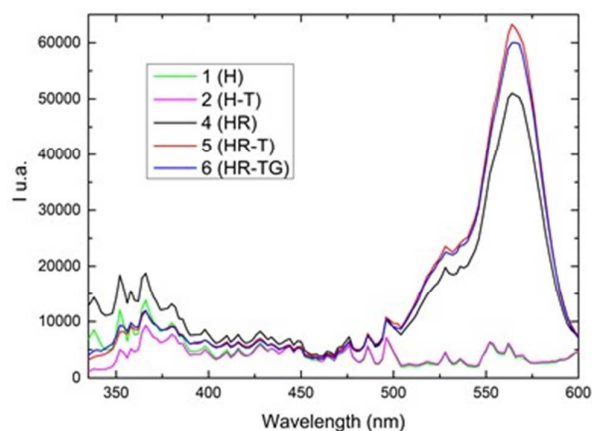


Figure S4. Excitation spectra in the range 330-600nm at $\lambda_{em} = 620$ nm of the **1 (H)**, **2 (H-T)**, **4 (HR)**, **5 (HR-T)** and **6 (HR-TG)**.

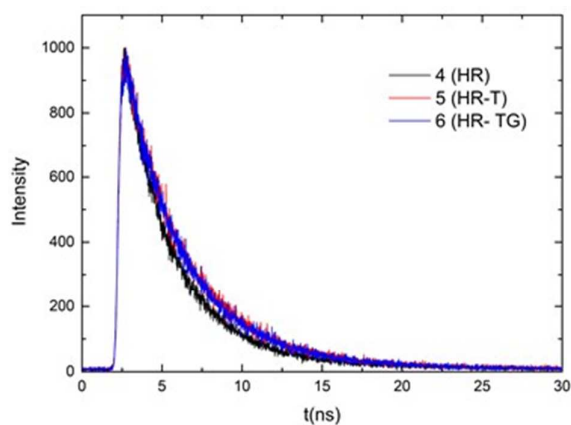


Figure S5. Comparison of the RhB emission lifetime decays in the ns timescale for **4 (HR)**, **5 (HR-T)** and **6 (HR-TG)**. The system is excited at $\lambda_{exc}=408$ nm with a detection at $\lambda_{em}=530$ nm.

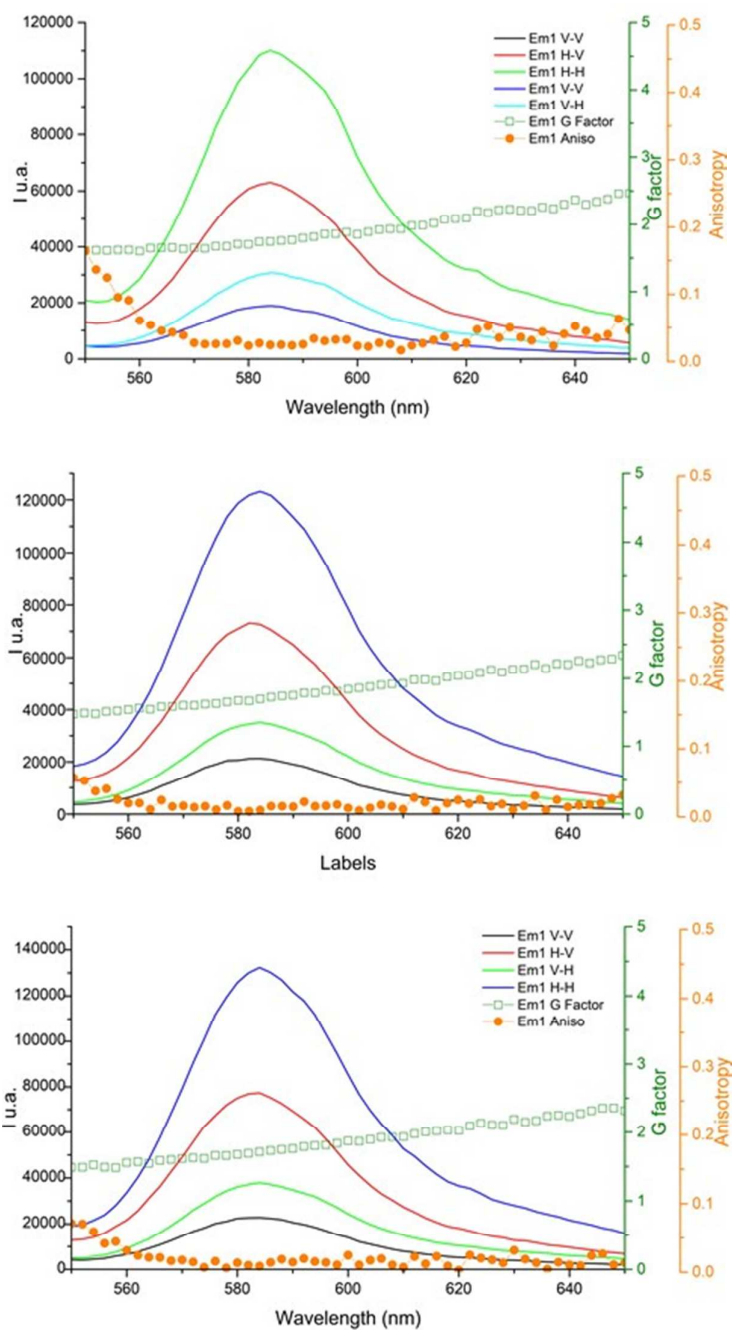


Figure S6. Fluorescence anisotropy measurements for the samples **4 (HR)**, **5 (HR-T)** and **6 (HR-TG)** (up to down). Continuous lines display Emission intensity collected with vertical (polarization of 0°), V, or horizontal (polarization of 90°, H, polarized excitation/ emission). The excitation was performed at 530 Square (green) dotted line display the G factor. The round (orange) dotted line is the anisotropy value.

Pseudo first order analysis of the photodegradation kinetics

In order to go more into the detail in the photo-degradation kinetics, we analysed the kinetics traces of Figure 6 according to a first (pseudo) first order model:

Eq.S1

$$c(t) = c_0 e^{-kt}$$

Where $c(t)$ is the concentration of **RhB** as a function of time, c_0 is the initial concentration of the dye and k the (pseudo) first order rate constant. Considered that, as mentioned, in the experimental conditions the fluorescence intensity $I(t)$ is proportional to $c(t)$ a linear dependency of $\ln(I(t)/I_0)$ from the time is expected according to equation:

Eq.S2

$$-\ln \frac{I(t)}{I_0} = kt$$

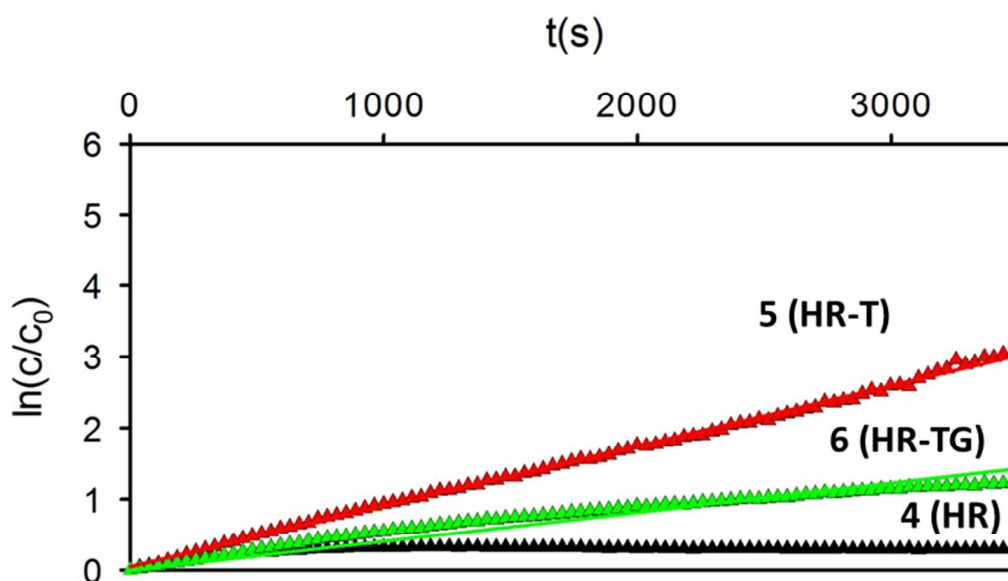


Figure S7 log plots of $c(t)/c_0$ versus t as measured for **4 (HR)**, **5 (HR-T)** and **6 (HR-TG)**. The plots were linearly fitted according to eq. S2 to give the rate constant k (in units of s^{-1}) that represent the lines slopes. From the data analysis we obtain values of $k = 8.0 \pm 0.1 \times 10^{-4} s^{-1}$ and $k = 4.0 \pm 0.1 \times 10^{-4} s^{-1}$ for **5 (HR-T)** and **6 (HR-TG)** respectively.

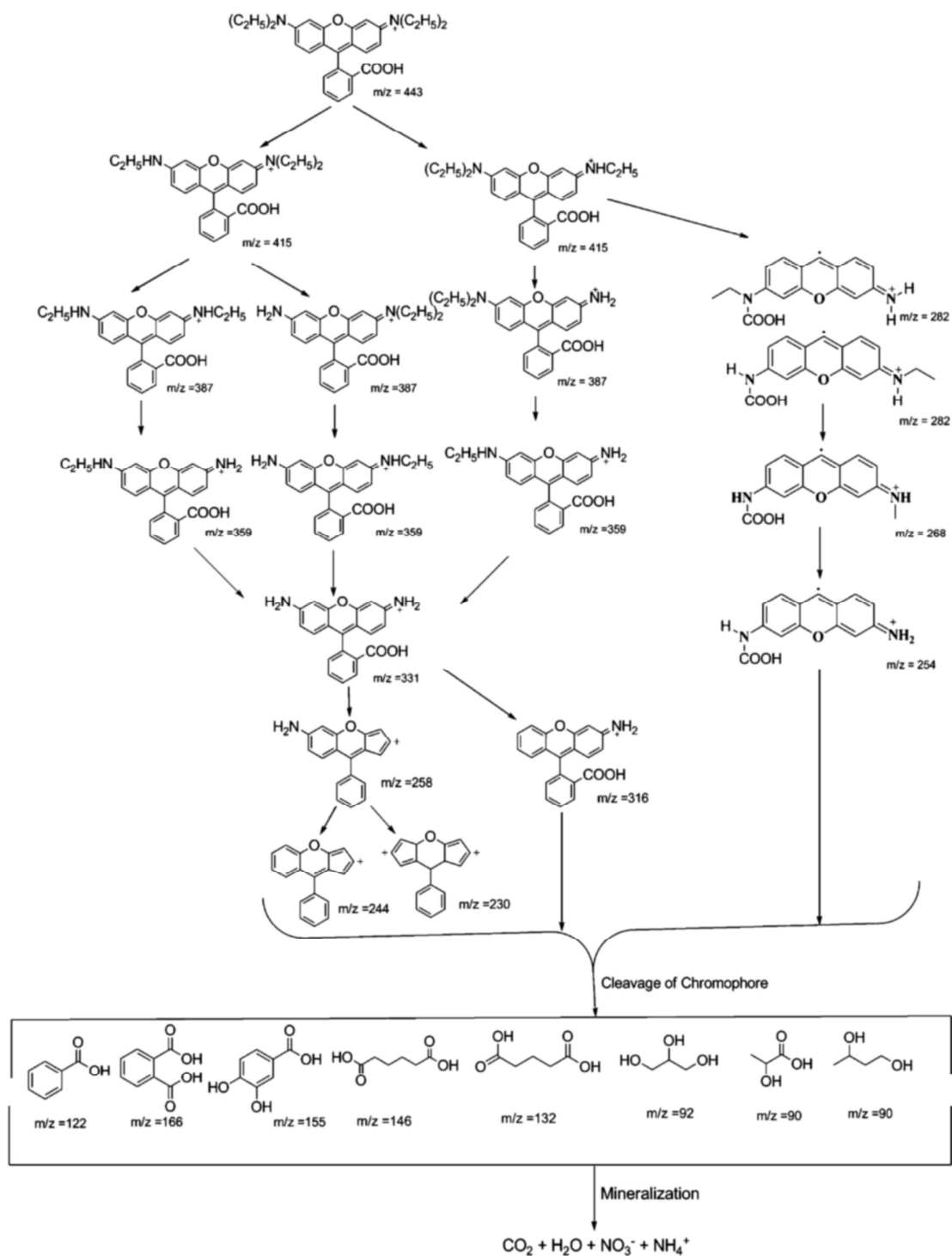


Figure S8. Hypothesis for the mechanism of RhB degradation pathway. The degradation leads to the disruption of the RhB dye aromatic system, that is responsible of the fluorescence signal.⁴ [4]

(4) Natarajan, T. S.; Thomas, M.; Natarajan, K.; Bajaj, H. C.; Tayade, R. J. Study on UV-LED/TiO₂ Process for Degradation of Rhodamine B Dye. *Chem. Eng. J.* **2011**, 169 (1), 126–134.